energy&fuels

Article

Behavior of Alkali Metals in Fly Ash during Waste Heat Recovery for Municipal Solid Waste Incineration (MSWI)

Jing Zhao, Xiaolin Wei, Teng Li, Huixin Li, and Feng Bin

Energy Fuels, **Just Accepted Manuscript** • DOI: 10.1021/acs.energyfuels.7b03001 • Publication Date (Web): 13 Nov 2017

ACS Publications

Energy & Fuels is published by the American Chemical Society. 1155 Sixteenth Street N.W., Washington, DC 20036

Behavior of Alkali Metals in Fly Ash during Waste Heat Recovery for Municipal Solid Waste Incineration (MSWI)

Jing Zhao[1,2], *Xiaolin Wei**[1,2], *Teng Li*[1], *Huixin Li*[1,2], *Feng Bin*[1]

1. State Key Laboratory of High-Temperature Gas Dynamics, Institute of Mechanics, Chinese Academy of Sciences, Beijing 100190, China

2. School of Engineering and Science, University of Chinese Academy of Sciences, Beijing 100049, China

Abstract: Fly ash containing high levels of alkali metals likely causes deleterious effects during municipal solid waste incineration (MSWI), including fouling, slagging, corrosion, and deterioration of materials. This study aimed to understand the occurrence of alkali metals in fly ash, the attachment phenomenon of fly ash and the corrosion mechanisms of high-temperature surfaces in heat exchangers. The presence of alkali metals was studied through a three-step extraction. Additionally, scanning electron microscopy-energy dispersive spectrometry (SEM-EDS) was used to analyze the surface microstructure of fly ashes. X-ray fluorescence (XRF) and X-ray diffraction (XRD) spectroscopy were used for content and crystalline phase analyses of alkali metals. The experimental results indicated that the surfaces of fly ash that contained higher levels of alkali metals were more smoother, and the content of alkali metals tended to increase with the slightly fluctuation with declining effluent gas temperature. The alkali metals were mainly water soluble. Based on the XRD analyses, the water-soluble alkali metals were primarily alkali chlorides and sulfates existing as NaCl, KCl and $K_3Na(SO_4)_2$. Moreover, the transformation of alkali metals could accelerate

corrosion of heat exchanger due to the formation of low temperature eutectic melt.

Key Words: Fly ash; Alkali metals; Municipal solid waste incineration; Occurrence; Transformation

Nomenclature

Abbreviation	Full name
MSW	municipal solid waste
MSWI	municipal solid waste incineration
PVC	polyvinylchloride
SEM-EDS	scanning electron microscopy-energy dispersive spectrometry
XRF	X-ray fluorescence
XRD	X-ray diffraction
RIR	reference intensity ratio
RSDs	relative standard deviations
FA	fly ash
Symbols	**Unit**
I	intensity (cps)
W	weight fraction (%)
M	relative atomic mass

1. Introduction

The treatment of MSW poses serious problems due to the rapid expansion of cities and urbanization of rural areas in China [1, 2]. The incineration of MSW has many advantages, including significant reductions in waste volume (approximately 70-90 %), energy recovery, and the complete disinfection and conversion of ash into building materials [3-5]. However, in terms of environmental considerations, MSWI faces serious challenges. During incineration, various solid residues, such as bottom ash, fly ash and particulates, are produced as secondary pollutants [6-8]. The unsorted MSWs typically incinerated in China include wood, glass, paper, kitchen waste and all kinds of plastic. Unsorted wood, PVC, and kitchen waste may create high concentrations of Na, K and Cl [9]. During MSWI, Na and K are generally released as NaCl and KCl, and, in the presence of sulfur in effluent gas, alkali metal sulfates are produced by the following reaction [10-12].

$$2MCl + 2SO_2 + 2O_2 + H_2O = M_2(SO_4)_2 + 2HCl \quad (M: Na, K)$$

Compared with alkali metal chlorides, sulfates are more stable. Generally, alkali metal sulfate formation requires higher temperatures [13]. Alkali metal chlorides and sulfates are more inclined to combine with fly ash when the gas temperature decreases during waste heat recovery [14-16].

Most studies have focused on heavy metals and have failed to address alkali metals during MSWI. High chloride concentrations, especially of NaCl and KCl, can decrease the melting temperatures of MSWI fly ashes and cause severe slagging and corrosion when the fly ashes that contain alkali metals deposit on high-temperature surfaces of heat exchangers during waste heat recovery [17, 18]. These problems endanger employees and increase the cost of facilities [19]. Therefore, research on alkali metals in MSWI fly ashes is urgently needed. Moreover, most reports have focused on the removal of alkali metals in fly ashes, and the attachment process of alkali metals on fly ashes has largely been ignored. During incineration, high temperatures can promote the release of alkali metals [20, 21]. Reductions in temperature in waste heat boilers can promote the attachment of alkali metals on fly ash [22-24]. The influence of temperature on alkali metal attachment should be studied to identify zones prone to corrosion. XRD analyses of the main crystalline phases of Na and K have been conducted by RIR method [25]. These quantitative studies can help in understanding the phase analyses of Na and K in fly ashes compared with qualitative analysis.

The occurrence modes and levels of alkali metals should be known in facility design and operation. Usually, these factors are determined by a sequential extraction method [26-28], which is a three-step procedure using three types of extraction solutions: deionized water, ammonium acetate (NH_4OAc) and hydrochloric (HCl). Accordingly, alkali metals are categorized into four occurrence modes: water soluble, exchangeable, acid soluble and acid insoluble. The alkali metal contents in each of the four occurrence modes are determined by analyzing extract solutions collected in each step [29]. Generally, alkali metal chlorides and sulfates that exist as water-soluble forms are more easily released during MSWI [30].

This paper reports on the laboratory-scale results of the study of MSWI fly ashes via four experimental methods, i.e., SEM-EDS, XRF spectroscopy, three-step extraction, and XRD spectroscopy. The surface microstructures of fly ashes were analyzed by SEM-EDS. Alkali metal content variations in fly ash were determined by XRF during waste heat recovery. Alkali metal occurrence modes and contents were determined by three-step extraction. XRD was used to study the detailed crystalline phases of alkali metals in fly ash. An alkali metal chloride corrosion mechanism on high-temperature surfaces of heat exchangers was also introduced.

2. Experimental Materials and procedures

2.1. Experimental materials

MSWI fly ashes, i.e., FA-1, FA-2, FA-3 and FA-4, were collected from a municipal solid waste incinerator plant (as shown in Figure 1a) located in Haikou, Hainan Province, China, which handles 600 tons of MSW (about 1.25-2.65 % alkali metals) per day and produces 54.5 tons/hour vapor. The fly ash samples were collected by an isokinetic sampling device and fly ash in the gas, could enter the sample bottle under gravity inertia through a cyclone separator. Samples as received were dried at relatively low temperatures (T<50 ℃) and sieved to particle sizes between 40 μm and 100 μm. The gas temperature of a receiving hopper is shown in Figure 1b and the corresponding position of temperature measurement can be found in Figure 1a. The contents of Na_2O, K_2O and SiO_2 in fly ashes are listed in Table 1. SiO_2 was used as a reference for XRD quantitative analysis. Obviously, MSW fly ashes were characterized by high Na and K.

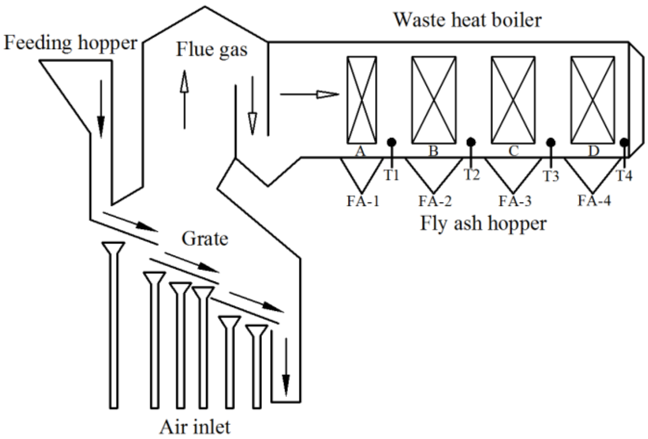

(a)

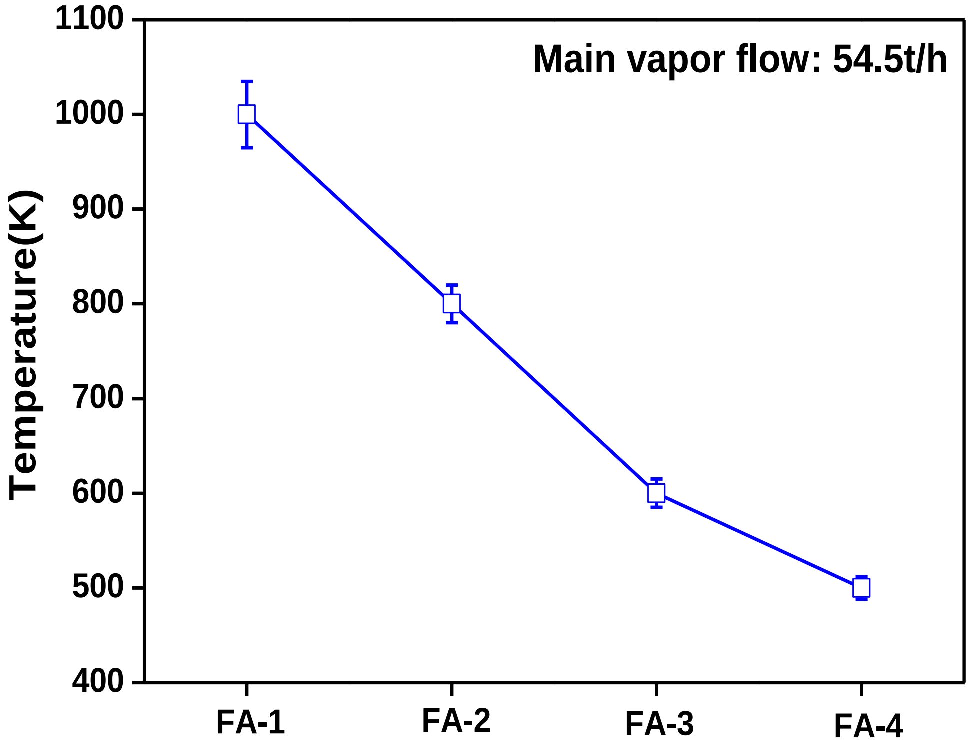

(b)

Figure 1. (a) Schematic of waste-to-energy facility located in Haikou, Hainan Province, China: A-flue gas preheater; B-superheater; C-vaporizer; D-economizer. (b) The gas temperature corresponding to hopper position.

Table 1 Contents of Na_2O, K_2O and SiO_2 in fly ash (mg/g)

Samples	Na_2O	K_2O	SiO_2
FA-1	31.7	23.3	35.4
FA-2	97.6	61.0	32.7
FA-3	185.9	85.2	31.6
FA-4	193.7	101.3	30.4

2.2. Experimental procedures

Prior to the experiments, all sieved fly ash samples were dried again in an oven at 383 K in a N_2 atmosphere for 2 h. The morphology and relative elemental contents of fly ash mixtures were determined using a scanning electron microscope (JSM-7800F, JEOL, Japan) and energy-dispersive X-ray spectroscopy (SEM-EDX) at an accelerating voltage of 20 kV. Fly ash sample contents were then analyzed by XRF using an energy-dispersive instrument (E3, Netherlands). Crystalline phase analyses were determined by powder XRD using a Rigaku D/MAC/max 2500 v/pc instrument (DX2700, China) with Cu-Kα radiation (40 kV, 200 mA, λ=1.5418 A). Diffractometer data were acquired at a step size of 0.02º for 2θ values from 5-80 º

A three-step sequential extraction of alkali metals was employed based on the method of Benson for low-rank coals [26]. For the water-soluble occurrence mode, 1 g of fly ash and 100 ml of deionized water were mixed in a 150 ml polyethylene centrifuge tube. The tube was placed in a 60 ℃ water bath for at least 24 h. The washing solution was collected for water-soluble Na and K analyses (denoted as Na_w and K_w, respectively). The residue was used for the next step. For the exchangeable occurrence mode, 100 ml of the 1 mol/L NH_4OAc buffer solution was added to the residue, and the above operation was repeated. Exchangeable Na and K were denoted as Na_{ex} and K_{ex}. For the acid-soluble occurrence mode, the procedure was the same as that used in determining the exchangeable occurrence mode, but the solution used for the residue was 1 mol/L HCl. The determined Na and K were acid soluble and were denoted as Na_{ac} and K_{ac}, respectively. The Na and K in the residue can be classified as insoluble and were denoted as Na_{ins} and K_{ins}, respectively. In each step, the dissolved Na and K species were measured by ICAP 6000 Series. The alkali metal contents were converted to fly ash weight base. At least three replicates of each sample were examined; relative standard deviations (RSDs) were less than 5 %.

3. Results and discussion

3.1 Morphology and composition of MSWI fly ashes

During waste heat recovery in MSWI, some alkali metals in the flue gas attach to the MSW fly ash as the temperature decreased from 1000 to 500 K. Figure 2 shows detailed images of fly ash morphology as provided by SEM. The compositions of the four fly ashes as determined by EDX analysis are also shown. The four fly ashes are characterized as high amounts of Ca, Na, K, Cl, S, et al elements. As determined by EDX in the FA-1 and FA-2 fly ashes, the positions of relative high Ca content were inhomogeneous and contained many needle-shaped crystallites and irregular materials, indicating the presence of chlorides and sulfates of Ca [30]. Comparatively, Na and K were enriched in the smother position in FA-3 and FA-4 fly ash samples, indicating the existence of chlorides and sulfates of Na and K.

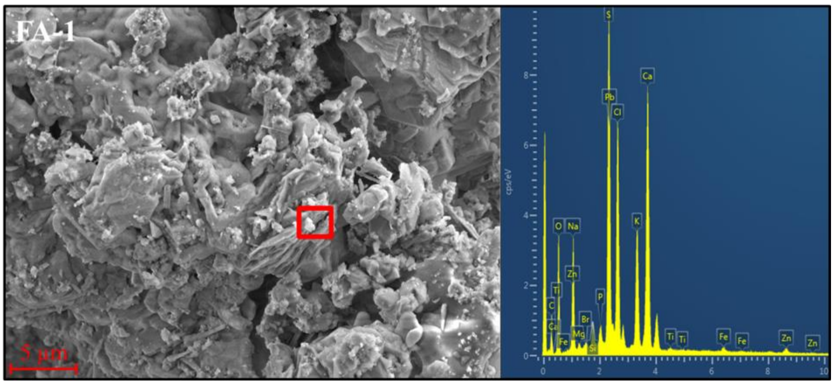

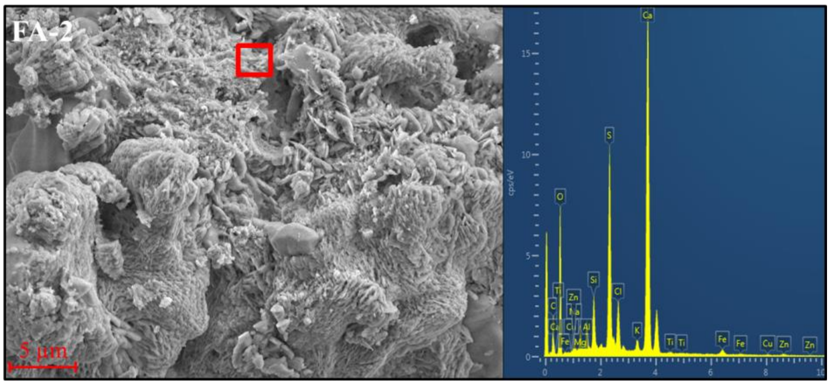

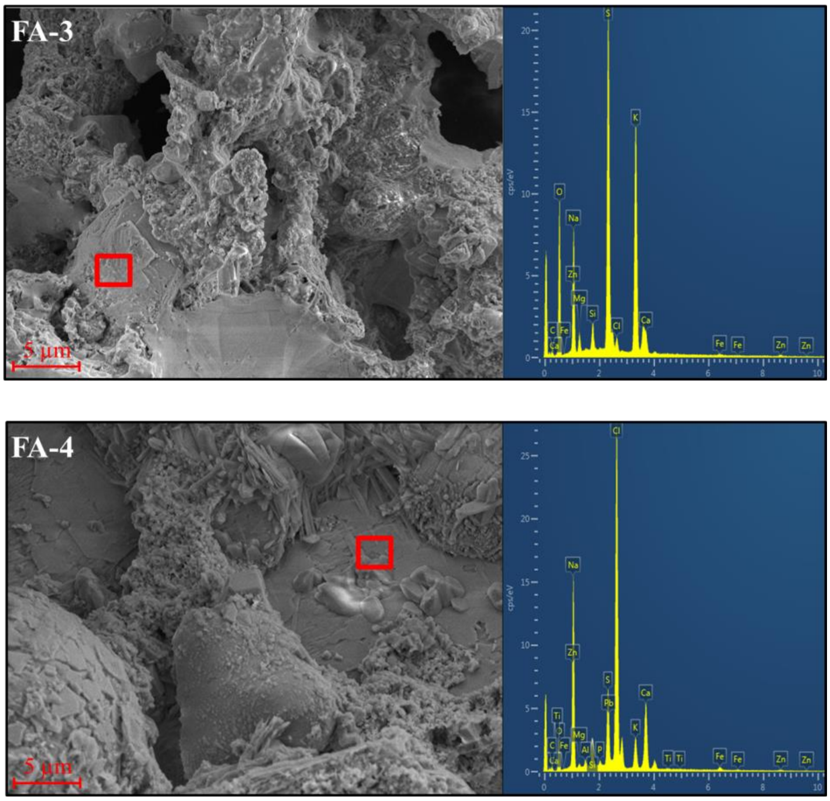

Figure 2. The results of SEM-EDS for four MSWI fly ashes

This phenomenon was consistent with the results obtained from XRF (see Figure 3), which indicated that the contents of alkali metals increased from the hoppers of FA-1 to FA-4. In the hopper of FA-1, the alkali metals in the fly ash were relatively low compared with those of the other hoppers. A large amount of alkali metals remained in gaseous form as Na(g) and K(g) or as aerosols because of the higher hopper temperatures. For FA-2, the Na mass fraction increased from 2.35 % to 6.74 % as the gas temperature decreased. The concentration of Na reached a maximum value of 12.87 % in FA-4. The total Na ratio in FA-4 increased by approximately 5.5-folds compared with that of FA-1. Fly ash variations in K were similar to those of Na during waste heat recovery. The K content increased from 1.94 % to 7.44 % with decreasing temperature. The results indicated that temperature had an important effect on the condensation of gaseous Na(g) and K(g) in fly ash. A reduction in flue gas temperature in the waste heat boiler can promote the enrichment of alkali metals in fly ashes. High amounts of alkali metals in fly ash could cause severe and harmful results, including fouling, slagging, corrosion, and deterioration of materials [9, 30].

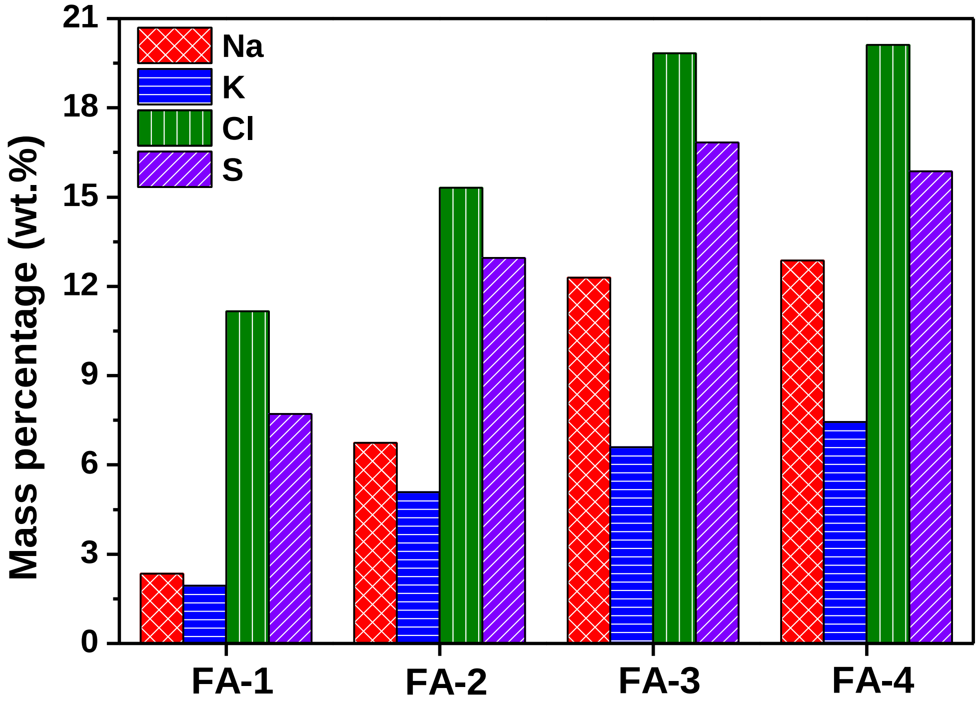

Figure 3. Contents of Na, K, Cl and S in four fly ashes

3.2 Occurrence modes of alkali metals in MSWI fly ashes

Figure 4 shows the total contents of Na and K determined in each extraction step (the stack column) and the total amount of Na_{total} and K_{total} in the fly ashes (denoted by asterisks). The experimental results showed that most of the Na and K in the fly ashes were water soluble. Compared with existing forms of water-soluble alkali metals, the number of Na and K of acid-soluble and insoluble alkali metals were relatively small. However, ammonium acetate soluble Na and K were not found in the fly ashes. The organic structures of alkali metals in fly ashes were destroyed under high temperature (>1273 K) during MSWI [31]. The contents of the water-soluble forms of Na and K increased sharply from 19.7 to 123.71 mg/g and 12.68 to 71.29 mg/g, respectively, as the temperature reduced during waste heat recovery. These results showed that Na and K in the flue gas were water soluble. The water-soluble Na and K were deposited on the fly ash particles as the temperature decreased. Acid-soluble and insoluble Na and K content variations were not obvious. This conclusion also indicated that small amounts of acid-soluble and insoluble Na and K were present when the fly ashes were initially formed and did not observably precipitate from the flue gas as the temperature decreased.

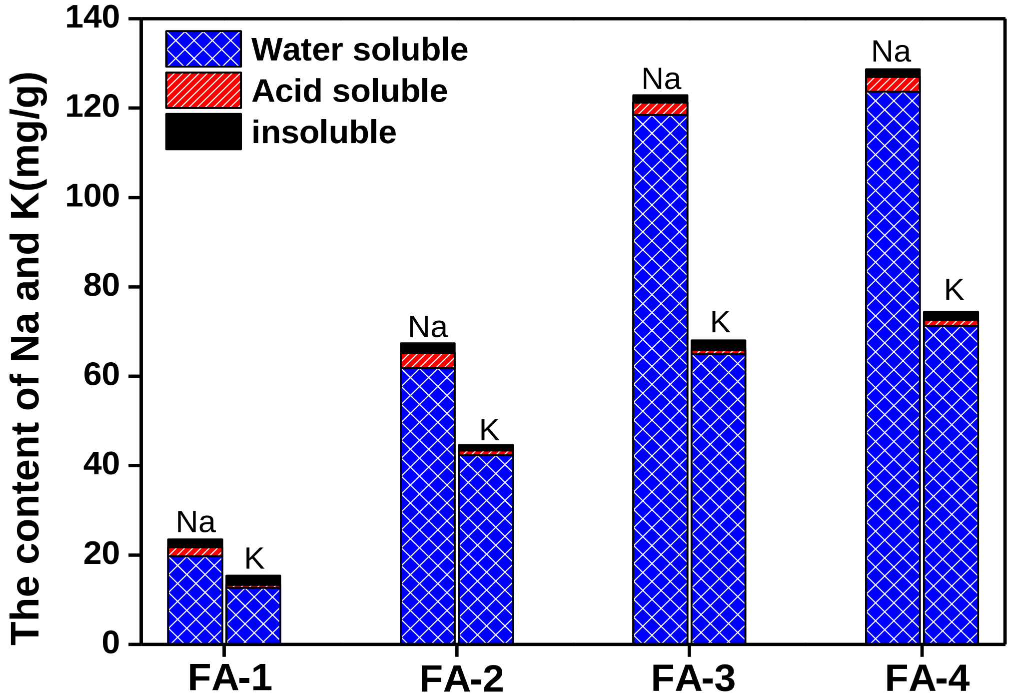

Figure 4. Summation of alkali metals contents using different extraction methods

3.3 Crystalline phase analysis of alkali metals in fly ashes

To investigate the detailed chemical compositions and compounds in the four fly ashes, XRD analyses were conducted to determine the main crystalline phases of the alkali metals. For the MSWI fly ashes, except FA-1, Na, K, Cl and S accounted for more than 40 % of the elements. As shown in Figure 5, high amounts of alkali metals, chlorine and sulfur indicated large amounts of alkali metal chlorides and sulfates, which were verified by XRD.

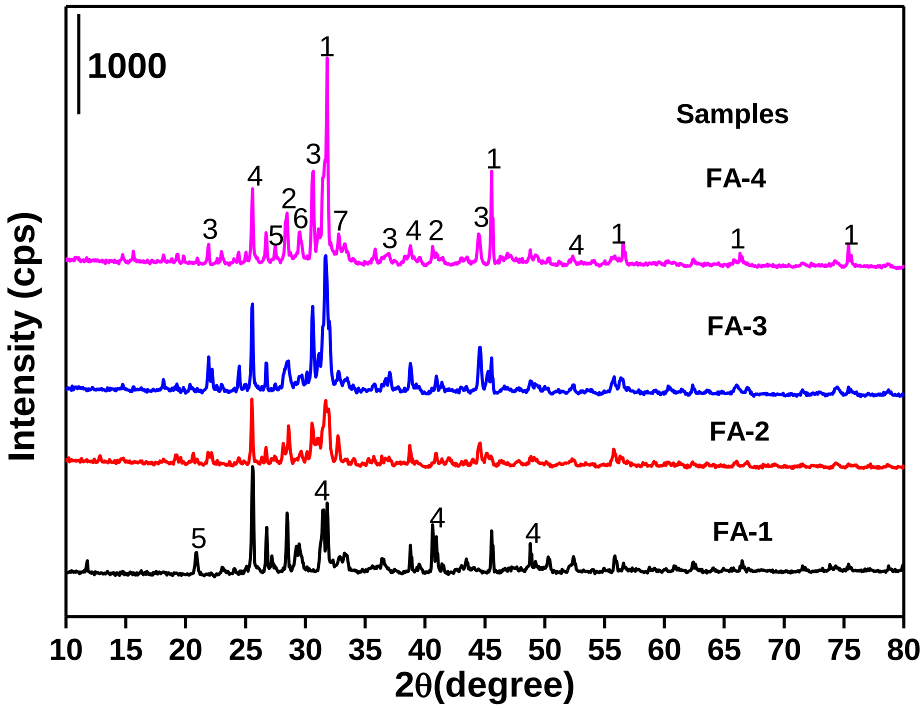

Figure 5. XRD pattern of four MSWI fly ashes, and the main crystalline phase can be shown as: 1 (Halite) NaCl; 2 (Sylvite) KCl; 3 (Potassium sodium salt) $K_3Na(SO_4)_2$; 4 (Anhydrite) $CaSO_4$; 5 (Quartz) SiO_2; 6 (Gehlenite) $Ca_2Al(AlSi)O_7$; 7 (Calcium hydroxide) $Ca(OH)_2$

Halite (NaCl), sylvite (KCl) and potassium sodium salt ($K_3Na(SO_4)_2$) made up the main alkali metal phases in the fly ashes. In FA-1, the Na and K crystalline phases were mainly alkali metal chlorides, such as NaCl and KCl, whereas alkali metal sulfate contents were relatively low. In FA-2, more alkali metal sulfates were found in the fly ash as $K_3Na(SO_4)_2$. Parts of NaCl and KCl were sulfated in the presence of SO_2 and SO_3 during MSWI. According to a few studies [32, 33], Na_2SO_4 forms when the temperature exceeds 1073 K. Considering the melting point of NaCl is 1074 K, that of KCl is 1043 K and that of $K_3Na(SO_4)_2$ is approximately 1157 K, when the combustion temperature exceeded 1157 K, the gaseous phase reaction played an important role during the sulfation of NaCl and KCl. The main reaction was as follows: NaCl(g) + 3KCl(g) +2H_2O(g) + 2SO_2(g) + O_2(g) =

$K_3Na(SO_4)_2$(g)+4HCl(g).

Concurrently, Figure 5 shows the band positions of NaCl, KCl and $K_3Na(SO_4)_2$ in the MSWI fly ashes. The NaCl bands were mainly found in peaks at 31.7 °, 45.6 °, 66.5 °and 75.4 °; the KCl bands showed peaks at 28.6 ° and 40.8 °; and the $K_3Na(SO_4)_2$ bands were characterized by peaks at 22 °, 30.6 °, 36.9 °and 44.5 °. The different bands of each crystalline phase indicated that the crystal structure planes were diverse, representing (2 0 0), (2 2 0), (4 0 0) and (4 2 0) for NaCl; (2 0 0) and (2 2 0) for KCl; and (1 0 1), (1 0 2), (0 0 3) and (0 2 2) for $K_3Na(SO_4)_2$. For XRD analyses, the absorbance band areas of each crystalline phase is related to their percentages [34]. The absorbance area of NaCl increased from FA-1 to FA-4 as the flue gas temperature reduced during waste heat recovery in the MSW incinerator. The main absorbance bands were characterized by peaks at 31.7 °and 45.6 °. This was the main reason that caused the Na content in fly ashes to increase as the waste heat recovery process proceeded. This was also observed for $K_3Na(SO_4)_2$, which had main absorbance peaks at 30.6 °and 44.5 °in addition to the main peak of FA-1 at 36.9 °. The absorption area of KCl was characterized by peaks at 28.6 °and 40.8 °as the gas temperature decreased. K content was enhanced due to contributions from $K_3Na(SO_4)_2$.

3.4 Quantitative analysis of crystalline phase in MSWI fly ashes

To further investigate the occurrence modes of halite (NaCl), sylvite (KCl) and potassium sodium salt ($K_3Na(SO_4)_2$), the XRD analyses of the four fly ashes were used to compare with PDF standards acting as a reference database. The RIR quantitative analysis for XRD is given by:

$$RIR_s^j = \frac{I_j}{I_s}\frac{W_j}{W_s}$$

where W denotes the weight fraction, I the intensity and the subscripts j and s indicate phase j and standard phases, respectively. For the corundum (Al_2O_3) standard phase, the intensity ratio was determined according to the most intense corundum line I_{cor} and the most intense line from phase j, I_j in a 1:1 mixture by weight. The RIR values are known as I/I_{cor} or RIR_{cor}. In terms of RIR_{cor} the concentrations of any phase j in a sample spiked with a known amount of corundum is given by:

$$W_j = \frac{W_{cor}}{RIR_{cor}} \frac{I_j}{I_{cor}}$$

The RIR_{cor} values for the main crystalline phases in the four MSWI fly ashes, determined from the spray-dried mixtures with corundum are listed in Table 2. The characteristic peak of corundum was not obvious in the XRD analysis; however, quartz was observed as characterized by a peak at 26.7 °. The weight fraction of quartz can be precisely measured by ash components analysis as shown in Table 1. The formula used to calculate the concentrations of any phase j can be converted as follows:

$$W_j = W_{qua} \frac{RIR_{cor}^{qua}}{RIR_{cor}^{j}} \frac{I_j}{I_{qua}}$$

Table 2 RIR_{cor} values of the main mineral in fly ashes, determined from spray-dried mixtures and corresponding peak positions

Mineral	Peak position (°)	Peak d-spacing (Å)	RIR_{cor}
Halite	31.7	2.82	4.71
Sylvite	28.6	3.14	6.07
Potassium sodium salt	30.6	2.84	2.39
Quartz	26.7	3.34	4.04

Considering the differences in diffraction peak widths for the crystalline phases in the fly ashes, the intensity ratios can be more accurately calculated by integral intensity (i.e., peak area) than linear intensity (i.e., peak height) [25]. The I_j/I_{qua} of NaCl, KCl and $K_3Na(SO_4)_2$ for the four MSWI fly ashes are shown in Table 3, and the mass fraction variations with decreasing temperature are shown in Figure 6. The mass fractions of NaCl and $K_3Na(SO_4)_2$ in the fly ashes tended to increase from FA-1 to FA-3 followed by slight fluctuations as the effluent gas temperature decreased. Compared with halite and potassium sodium salt, the KCl weight fraction variations were relatively stable. These results indicated that the alkali metals in the fly ashes separated from the flue gas in the crystalline phase formed NaCl and $K_3Na(SO_4)_2$. The sulfation of KCl can be considered the primary reason that the content of KCl slightly varied with decreasing gas temperature. Quantitative analyses of alkali metals can help us study the condensation of alkali metals in fly ashes. Higher Na and K contents in the input waste fed into the grate incinerator may partially result in high concentrations of Na and K in the fly ashes. In grate incinerators, alkali metals are primarily transformed to fly ashes by evaporation and condensation [35]. Generally, the mass fraction of alkali metals in fly ashes will be determined by the local temperature in the waste heat boiler.

Table 3 Ratio of the integral intensity between the crystalline phase of alkali metals and quartz

Phase	FA-1	FA-2	FA-3	FA-4
NaCl	1.57	4.72	8.43	10.53
KCl	1.12	1.65	1.83	1.98
$K_3Na(SO_4)_2$	0.22	1.73	2.24	2.43

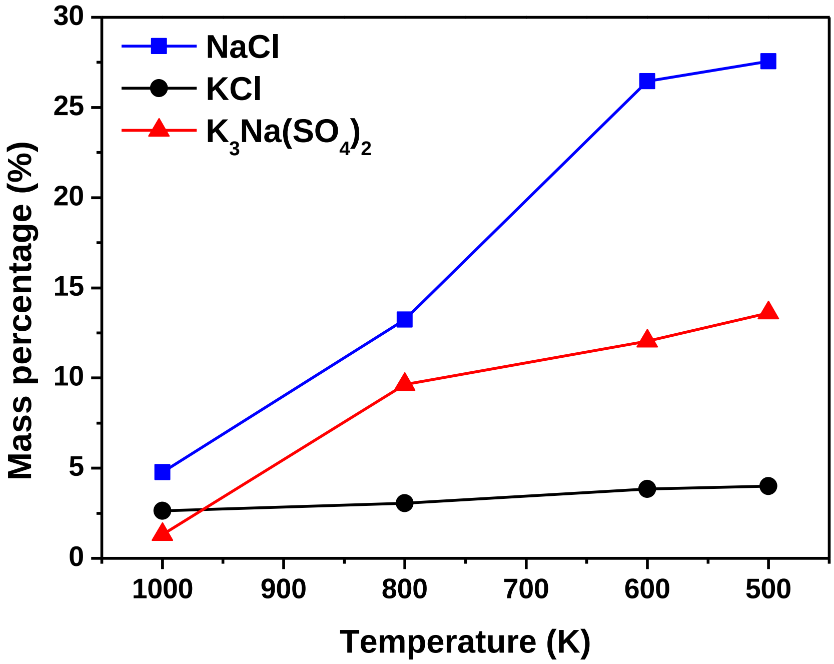

Figure 6. The influence of the gas temperature on the mass fraction of the main crystalline phase of water-soluble alkali metals in fly ashes

The accuracy of the quantitative XRD in the crystalline phase analysis of MSWI fly ashes was verified by comparing between XRD and XRF by calculating the weight fractions of water-soluble Na and K as follows:

$$W_{Na} = W_{hal}\frac{M_{Na}}{M_{hal}} + W_{pot}\frac{M_{Na}}{M_{pot}}$$

$$W_{K} = W_{syl}\frac{M_{K}}{M_{syl}} + W_{pot}\frac{M_{K}}{M_{pot}}$$

where M represents the relative atomic mass: M_{Na}=22.99, M_{K}=39.1, M_{Cl}=35.45, M_{S}=32.06 and M_{O}=16. The water-soluble alkali metals were assumed to consist of NaCl, KCl and $K_3Na(SO_4)_2$. Figure 7 illustrates the total water-soluble Na and K contents as determined by XRF and XRD, respectively. The results gained from XRF were consistent with those of XRD. This also showed that the water-soluble alkali metals mainly comprised chlorides and sulfates.

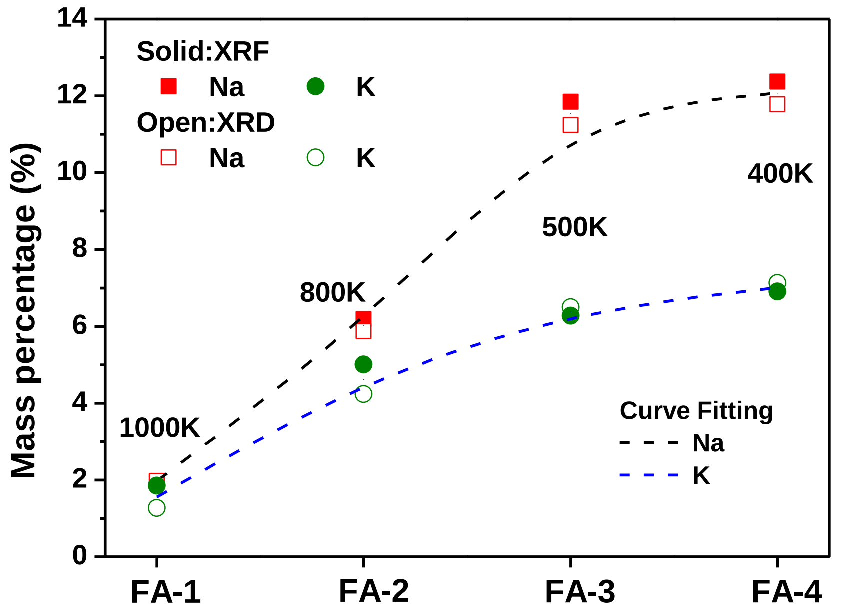

Figure 7. Comparison of alkali metals contents of water-soluble alkali metals determined by XRF and XRD

3.5 Analysis of the transformation of alkali metals during MSWI

Based on some conclusions provided by other researchers and our results, the release and migration paths of alkali metals can be predicted during MSWI, as shown in Figure 8. At the beginning of MSWI, sodium and potassium are released from MSW as gaseous metallic sodium, NaCl and KCl [10]. In the oxidizing atmosphere, in which SO_2 is present and the temperature reached 1157 K, NaCl and KCl reacted with SO_2 to form the gaseous alkali metal sulfate, $K_3Na(SO_4)_2$. When fly ash and gaseous alkali metals, such as NaCl, KCl and $K_3Na(SO_4)_2$, leave the grate incinerator and enter the waste heat boiler, the gas temperature decreases, and the alkali metals vapor or aerosols condense onto the fly ash, thereby decreasing the fly ash melting point and enhancing the corrosion and cohesiveness of fly ashes [8, 22]. The speculated mechanism determined with lab-scale experiments is similar to Otsuka [22] and Song, et al [31] and suitable for the occasion that the temperature plays a dominant role in the condensation of alkali metals on fly ashes.

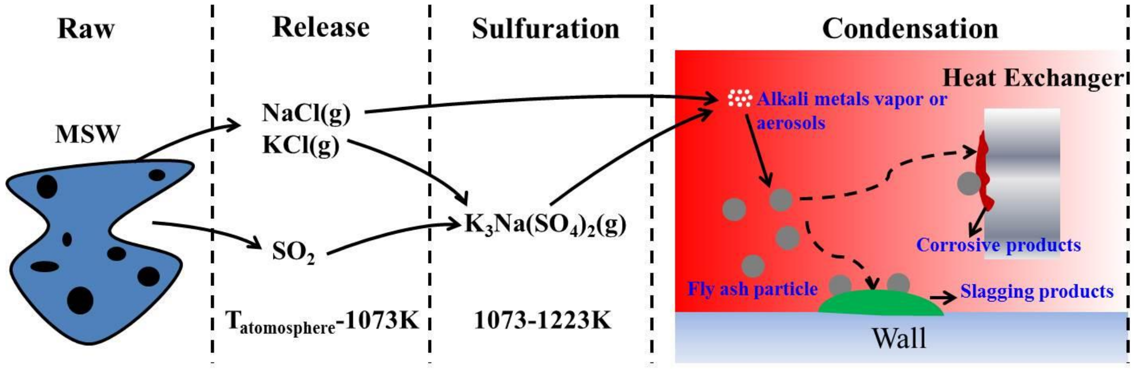

Figure 8. Mechanism of Na and K transformation, condensation and corrosion

To prevent corrosion of oxidation, the heat exchanger and chimney materials in some particular positions, are typically stainless steel in MSWI plants. Stainless steel consists of Fe, Cr and Ni. When fly ashes move to the surfaces of heat exchangers and chimney, alkali metals can accelerate the corrosion process due to the formation of low temperature eutectic melts. For example, Sulfate and chloride salts in MSWI fly ashes concentrate on protective metal oxide scales as Cr_2O_3 and Fe_2O_3 and become partially fused because these deposits contain alkali metals (Na and K) [22, 36]. Shinata [37] found that the oxidation rate of chromium was accelerated by NaCl. Below the melting points of NaCl and Na_2CrO_4, a low temperature eutectic melt was formed as NaCl-Na_2CrO_4 (melting point of 830 K). At the same time, NaCl-KCl-$FeCl_3$ can also form a eutectic melt system, accelerating corrosion [38, 39]. As a result, a dense, protective scale cannot be formed in the melt.

4. Conclusion

(1) As the temperature decreased from 1000 to 500 K during waste heat recovery, the alkali metal contents in the fly ashes gradually increased followed by slight fluctuations. The surfaces of fly ash that contained higher levels of alkali metals were more homogenous and smoother.

(2) The alkali metals primarily presented water-soluble occurrence modes as NaCl, KCl and $K_3Na(SO_4)_2$, as determined by crystalline phase analysis results from XRD. Quantitative analysis indicated that the increased fly ash Na content was due to the condensation of a large number of gaseous NaCl and the enhanced K content for $K_3Na(SO_4)_2$.

(3) When fly ash and gaseous alkali metals, such as NaCl, KCl and $K_3Na(SO_4)_2$, leave the grate incinerator and enter the waste heat boiler, the gas temperature decreases, and alkali metals vapor or aerosols condense onto the fly ash, decreasing the fly ash melting point and enhancing the corrosion and cohesiveness of fly ashes.

Corresponding Author

Email address: xlwei@imech.ac.cn (Prof. Dr. Xiaolin Wei).

Funding Sources

National Key R&D Program of China (2016YFB0601501)

Acknowledgements

Financial support for this work was from the National Key R&D Program of China (2016YFB0601501). The authors also thank for the suggestion of Mr. Running Kang on this work.

References

(1) Chen, X. D.; Geng, Y.; Fujita T. An overview of municipal solid waste management in China. *Waste Manage.* **2010**, *30*, 716-724.

(2) Cheng, H. F.; Hu, Y. A. Municipal solid waste (MSW) as a renewable source of energy: current and future practices in China. *Bioresour. Technol.* **2010**, *101*, 3816-3824.

(3) Kirby, C. S.; Rimstidt, J. D. Mineralogy and surface properties of municipal solid waste ash. *Environ. Sci. Technol.* **1993**, *27*, 652-660.

(4) Hjelmar, O. Disposal strategies for municipal solid waste incineration residues. *J. Hazard. Mater*. **1996**, *47*, 345-368.

(5) Yan, W. J.; Zhou, H. C.; Jiang, Z. W.; Lou C.; Zhang, X. K.; Chen, D. L. Experiments on measurement of temperature and emissivity of municipal solid waste (MSW) combustion by spectral analysis and image processing in visible spectrum. *Energy Fuels* **2013**, *27*, 6754-6762.

(6) Hamernik, J. D.; Frantz, G. C. Physical and chemical properties of municipal solid waste fly ash. *ACI Mater. J.* **1991**, *88*, 294-301.

(7) Davidsson, K. O.; Amand, L. E.; Leckner, B. Potassium, chlorine, and sulfur in ash, particles, deposits, and corrosion during wood combustion in a circulating fluidized-bed boiler. *Energy Fuels* **2007**, *21*, 71-81.

(8) Yu, J.; Sun, L. S.; Xiang, J. Jin, L. M.; Hu, S.; Su, S.; Qiu, J. R. Physical and chemical characterization of ashes from a municipal solid waste incinerator in China. *Waste Manage. Res*. **2013**, *31*, 663-673.

(9) Lebel, F.; Rapin, C.; Mareche, J. F.; Podor, R.; Chaucherie, X.; Guernion, P. Y.; Brossard, J. M. Development of a laboratory-scale pilot for studying corrosion on MSWI heat exchangers. *Mater. Sci. Forum* **2008**, *595-598*, 271-280.

(10) Abbas, Z.; Moghaddam, A.P.; Steenari, B.M. Release of salts from municipal solid waste combustion residues. *Waste Manage.* **2003**, *23*, 291-305.

(11) Liu, S.; Qiao, Y.; Lu, Z. L.; Gui, B.; Wei, M. M.; Yu, Y.; Xu, M. H. Release and

transformation of sodium in kitchen waste during torrefaction. *Energy Fuels* **2014**, *28*, 1911-1917.

(12) Lith, S. C. V.; Alonso-Ram ŕez, V.; Jensen, P. A.; Frandsen, F. J.; Glarborg, P. Release to the gas phase of inorganic elements during wood combustion. Part 1: Development and evaluation of 1uantification methods. *Energy Fuels* **2006**, *20*, 964-978.

(13) Iisa, K.; Lu, Y. P.; Salmenoja K. Sulfation of potassium chloride at combustion conditions. *Energy Fuels* **1999**, *13*, 1184-1190.

(14) Gallagher, N. B.; Bool L. E.; Wendt, J. O. L.; Peterson, T. W. Alkali metal partitioning in ash from pulverized coal combustion. *Combust. Sci. and Technol*. **1990**, *74*, 211-221.

(15) Zhou, H.; Zhou, B.; Zhang H. L.; Li, L. T.; Cen, K. F. Investigation of slagging characteristics in a 300 kW test furnace: effect of deposition surface temperature. *Ind. Eng. Chem. Res.* **2014**, *53*, 7233–7246.

(16) Wang, Y. B.; Tan, H. Z.; Wang, X. B.; Cao, R. J.; Wei, B. The condensation and thermodynamic characteristics of alkali compound vapors on wall during wheat straw combustion. *Fuel* **2017**, 187, 33-42.

(17) Werther, J.; Saenger M.; Hartge, E. U.; Ogada, T.; Siagi, Z. Combustion of agricultural residues. *Prog. Energy Combust. Sci.* **2000**, *26*, 1-27.

(18) Masi á, A. A. T.; Buhre, B. J. P.; Gupta R. P.; Wall, T. F. Characterising ash of biomass and waste. *Fuel Process. Technol.* **2007**, *88*, 1071-1081.

(19) Krause, H. H.; Wright, I. G. Boiler tube failures in municipal waste-to-energy plants. *Mater. Performance* **1996**, *35*, 16-53.

(20) Dayton, D. C.; Jenkins, B. M.; Turn, S. Q.; Bakker, R. R.; Williams, R. B.; Belle-Oudry,

D.; Hill, L. M. Release of inorganic constituents from leached biomass during thermal conversion. *Energy Fuels* **1999**, *13*, 860-870.

(21) Cheng, S.; Qiao, Y.; Huang, J. C.; Cao, L. W.; Yang, H. Z.; Liu, H.; Yu, Y.; Xu, M. H. Effect of alkali addition on sulfur transformation during low temperature pyrolysis of sewage sludge. *Proc. Combust. Inst.* **2017**, *36*, 2253-2261.

(22) Otsuka, N. A thermodynamic approach on vapor-condensation of corrosive salts from flue gas on boiler tubes in waste incinerators. *Corros. Sci.* **2008**, *50*, 1627-1636.

(23) Spiegel, M. Salt melt induced corrosion of metallic materials in waste incineration plants. *Mater. Corros.* **1999**, 50, 373-393.

(24) Krause, H. H. High temperature corrosion problems in waste incineration systems. *J. Mater. Energy Syst.* **1986**, 7, 322-332.

(25) Hillier S. Accurate quantitative analysis of clay and other minerals in sandstones by XRD: comparison of a Rietveld and a reference intensity ratio (RIR) method and the importance of sample preparation. *Clay Miner.* **2000**, *35*, 291-302.

(26) Benson, S. A.; Holm, P. L. Comparison of inorganics in three low-rank coals. *Ind. Eng. Chem. Prod. Res. and Dev.* **1985**, *24*, 145-149.

(27) Finkelman, R. B.; Palmer, C. A.; Krasnow, M. R.; Aruscavage, P. J.; Sellers, G. A.; Dulong, F. T. Combustion and leaching behavior of elements in the argonne premium coal samples. *Energy Fuels* **1990**, *4*, 755-766.

(28) Li, C. Z.; Sathe, C.; Kershaw, J. R.; Pang Y. Fates and roles of alkali and alkaline earth metals during the pyrolysis of a Victorian brown coal. *Fuel* **2000**, *79*, 427-438.

(29) Yang, Y. M.; Wu, Y. X.; Zhang, H.; Zhang, M.; Liu, Q.; Yang, H. R.; Lu, J. F. Improved

sequential extraction method for determation of alkali and alkaline earth metals in Zhundong coals. *Fuel* **2016**, 181, 951-957.

(30) Yu, J.; Qiao, Y.; Jin, L. M.; Ma, C.; Paterson, N.; Sun, L. S. Removal of toxic and alkali/alkaline earth metals during co-thermal treatment of two types of MSWI fly ashes in China. *Waste Manage.* **2015**, *46*, 287-297.

(31) Song, G. L.; Song, W. J.; Qi, X. B.; Lu, Q. G. Transformation characteristics of sodium of Zhundong coal combustion/gasification in circulating fluidized bed. *Energy Fuels* **2016**, *30*, 3473-3478.

(32) Vuthaluru, H. B.; Wall, T. F. Ash formation and deposition from a Victorian brown coal—modelling and prevention. *Fuel Process. Technol*. **1998**, *53*, 215-233.

(33) Tomeczek, J.; Palugniok, H.; Ochman, J. Modelling of deposits formation on heating tubes in pulverized coal boilers. *Fuel* **2004**, *83*, 213-221.

(34) Arvelakis, S.; Folkedahl, B.; Dam-Johansen, K.; Hurley, J. Studying the melting behavior of coal, biomass, and coal/biomass ash using viscosity and heated stage XRD data. *Energy Fuels* **2006**, *20*, 1329-1340.

(35) Yu, J.; Sun, L. S.; Xiang, J.; Jin, L. M.; Song, X.; Su, S.; Qiu, J. R. Physical and chemical characterization of ashes from a municipal solid waste incinerator in China. *Waste Manage. Res.* **2013**, *31*, 663-673.

(36) Brossard, J. M.; Diop, I.; Chaucherie, X.; Nicol, F.; Rapin, C.; Vilasi, M. Superheater fireside corrosion mechanisms in MSWI plants: Lab-scale study and on-site results. *Mater. Corros*. **2011**, *62*, 543-548.

(37) Shinata, Y. Accelerated oxidation rate of chromium induced by sodium chloride. *Oxid.*

Met. **1987**, *27*, 315-332.

(38) Rapp, R. A.; Devan, J. H.; Douglass, D. L. High temperature corrosion in energy systems. *Mater. Sci. Eng.* **1981**, *50*, 1-17.

(39) Ihara,Y.; Ohgame, H.; Sakiyama, K.; Hashimoto, K. ChemInform Abstract: The corrosion behavior of chromium in hydrogen chloride gas and gas mixtures of hydrogen chloride and oxygen at high temperatures. *Chem. Inform.* **1983**, *23*, 167-181.